

Hoxa2 and *Hoxb2* Control Dorsoventral Patterns of Neuronal Development in the Rostral Hindbrain

Marc Davenne,* Mark K. Maconochie,† Rüdiger Neun,* Alexandre Pattyn,‡ Pierre Chambon,* Robb Krumlauf,† and Filippo M. Rijli*§

*Institut de Génétique et de Biologie Moléculaire et Cellulaire
Centre National de la Recherche Scientifique/Institut National de la Santé et de la Recherche Médicale/Université Louis Pasteur
Collège de France
BP 163-67404 Illkirch Cedex Strasbourg
France

†Laboratory of Developmental Neurobiology
Medical Research Council
National Institute for Medical Research
London NW7 1AA
United Kingdom

‡Institut de Biologie du Développement de Marseille
Centre National de la Recherche Scientifique/Institut National de la Santé et de la Recherche Médicale/Université de la Méditerranée
F-13288 Marseille Cedex 9
France

Summary

Little is known about how the generation of specific neuronal types at stereotypic positions within the hindbrain is linked to *Hox* gene-mediated patterning. Here, we show that during neurogenesis, *Hox* paralog group 2 genes control both anteroposterior (A-P) and dorsoventral (D-V) patterning. *Hoxa2* and *Hoxb2* differentially regulate, in a rhombomere-specific manner, the expression of several genes in broad D-V-restricted domains or narrower longitudinal columns of neuronal progenitors, immature neurons, and differentiating neuronal subtypes. Moreover, *Hoxa2* and *Hoxb2* can functionally synergize in controlling the development of ventral neuronal subtypes in rhombomere 3 (r3). Thus, in addition to their roles in A-P patterning, *Hoxa2* and *Hoxb2* have distinct and restricted functions along the D-V axis during neurogenesis, providing insights into how neuronal fates are assigned at stereotypic positions within the hindbrain.

Introduction

Understanding how the mammalian central nervous system (CNS) is patterned into functionally distinct areas and how cellular diversity is generated are important issues. Distinct neuronal types differentiate at specific positions within the developing neural tube in response to signals along the anteroposterior (A-P) and dorsoventral (D-V) axes. Several studies have established a

link between the location of neural progenitors and their commitment to a specific fate (Simon et al., 1995; Itasaki et al., 1996; Grapin-Botton et al., 1997; Ye et al., 1998).

Recently, genetic pathways controlling positional information along the vertebrate A-P and D-V neural axes (Lumsden and Krumlauf, 1996; Tanabe and Jessell, 1996) and those controlling neurogenesis and neuronal differentiation have been uncovered. *Hox* and *Pax* transcription factors show spatially restricted expression during early neurogenesis and appear to be required for the readout of A-P and D-V identities, respectively (Goddard et al., 1996; Studer et al., 1996, 1998; Ericson et al., 1997; Gavalas et al., 1997, 1998; Osumi et al., 1997; Tiret et al., 1998). Furthermore, vertebrate homologs of the *Drosophila* basic helix-loop-helix (bHLH) *achaete-scute* (*ac-sc*) and *atonal* LIM- and homeodomain proteins are expressed in specific pools of neuronal precursors or developing neurons and control determination and/or differentiation of neuronal types (e.g., Kageyama and Nakanishi, 1997; Pfaff and Kintner, 1998). Interestingly, specific changes in *Hox* expression occur along the D-V axis of the spinal cord in relation to the birth of major classes of neurons (Graham et al., 1991), suggesting cross-talk between A-P, D-V, and neurogenic patterning. However, little is known about how A-P and D-V positional information is integrated and impinges on neurogenesis to generate discrete neuronal patterns.

The vertebrate hindbrain is a suitable system for studying the genetic and cellular mechanisms controlling patterns of neuronal specification and differentiation. It is transiently partitioned into compartments, the rhombomeres, which behave as lineage restriction units (Fraser et al., 1990), and each rhombomere generates similar repertoires of neurons (Clarke and Lumsden, 1993). However, the number, distribution, and specialization of neurons are rhombomere specific (Clarke and Lumsden, 1993), illustrating that positional information along the A-P axis may determine neuronal phenotype. The segmental organization is particularly evident for reticular neurons, vestibulo-acoustic efferent neurons, and the branchiomotor neurons of the cranial nerves (Marshall et al., 1992; Carpenter et al., 1993; Clarke and Lumsden, 1993; Simon and Lumsden, 1993). Moreover, the timing of neurogenesis is closely linked to A-P position; neurons in odd numbered rhombomeres are generated later than even numbered rhombomeres (Lumsden and Keynes, 1989). Rhombomere-specific specialization of neuronal types is also evident. Mouse rhombomere 2 (r2) branchiomotor neurons migrate dorsally from a ventral position to form the Vth (trigeminal) motor nucleus, whereas r4 branchiomotor neurons migrate posteriorly into r5 and r6, where they eventually form the VIIIth (facial) motor nucleus in a ventral location (Auclair et al., 1996; Studer et al., 1996; McKay et al., 1997).

While A-P position may determine identity within a given class of neurons, D-V positional values may control generic fate choices (e.g., motor neuron versus interneuron). Recent studies (Ericson et al., 1997) suggest that D-V fates in the hindbrain may be specified by mechanisms similar to those generating cell diversity

§To whom correspondence should be addressed (e-mail: rijli@igbmc.u-strasbg.fr).

in the spinal cord (Tanabe and Jessell, 1996). Distinct classes of neurons are generated at specific D-V positions and are influenced by local signals that regulate *Pax* expression in precursor pools. In the specification of motor neuron and ventral interneuron identities, *Pax6* is an essential mediator of *Sonic Hedgehog* (*Shh*) activity derived from the notochord and floor plate (fp) (Ericson et al., 1997). Dorsalizing signals from the surface ectoderm and roof plate may induce specification of dorsal cell types. In the hindbrain, positional identity is not conferred to multipotent precursors simultaneously along the A-P and D-V axes; A-P values appear to become fixed before D-V ones (Simon et al., 1995). Limited dispersal of precursors along the D-V axis (Clarke et al., 1998) may limit exposure to extrinsic signals and underlie the apparent early restriction of fate suggested by lineage analysis (Lumsden et al., 1994). These and recent experiments (Ye et al., 1998) suggest that cells are committed to their fates according to their position on an orthogonal grid of coordinates, where they independently respond to signals acting along both the A-P and D-V axes of the early neural tube. However, these data do not provide insights as to how the A-P and D-V positional addresses are integrated at the molecular level in precursor cells to generate and maintain specific neuronal phenotypes.

Mutational analysis of several transcription factors with rhombomere-specific expression patterns has demonstrated their function in controlling segmentation and A-P patterning. *Krox-20* is expressed before morphological segmentation in the presumptive r3 and r5 territories, where it activates *Hoxa2* and *Hoxb2* (Sham et al., 1993; Nonchev et al., 1996). In *Krox-20*^{-/-} embryos, r3 and r5 form but are progressively eliminated, which then also alters the development of even numbered rhombomeres (Schneider-Maunoury et al., 1997). *Hox* genes are involved in several aspects of segmental patterning (Rijli et al., 1998). Ectopic *Hoxa1* expression in mouse hindbrains results in r2 gaining r4 features (Zhang et al., 1994), while partial deletions of r4 and r5 are observed in *Hoxa1*^{-/-} embryos, suggesting an early role in segment formation (Carpenter et al., 1993; Mark et al., 1993). *Hoxb1*^{-/-} embryos show altered development of r4 branchiomotor neurons and migratory defects, with a normal number of segments (Goddard et al., 1996; Studer et al., 1996). Recently, we have shown that *Hoxa1* and *Hoxb1* are also required to initiate r4 specification and to pattern r4-derived neural crest (Gavalas et al., 1998; Studer et al., 1998). While these studies indicate an important role for *Hox* genes in several aspects of A-P patterning in hindbrain development, they do not address the link between *Hox*-mediated patterning and metamerism neurogenesis.

Here, we investigate the mechanisms regulating neuronal fate downstream of *Hoxa2* and *Hoxb2*. We previously showed that molecular and morphological aspects of r2 and r3 patterning are altered in *Hoxa2*^{-/-} mutants (Gavalas et al., 1997). Here, we generated a *Hoxb2*-targeted mutation and analyzed single and double *Hoxa2*^{-/-}/*Hoxb2*^{-/-} mutants to assess the function of these genes in early neurogenesis. While r3–r5 segmentation appears normal, we revealed a requirement in patterning interrhomomere boundaries. Moreover, *Hoxa2* and *Hoxb2* have distinct and restricted functions along both the A-P and the D-V axes during hindbrain neurogenesis.

Results

Normal r3–r5 Segmentation in Single and Double Mutants

To investigate the genetic interactions between *Hoxa2* and *Hoxb2* in hindbrain development, we generated *Hoxb2* mutant mice for mating with our *Hoxa2* mutant line (Figure 1). Since *Krox-20* is required to maintain r3 and r5 and directly regulates *Hoxa2* and *Hoxb2* in these segments, we first asked whether *Hoxa2*^{-/-}/*Hoxb2*^{-/-} mutant embryos lacked r3 and r5. In single and double mutants, we analyzed the segmental expression of *Krox-20* and of its direct target receptor tyrosine kinase *EphA4* (Theil et al., 1998) by whole-mount in situ hybridization and immunostaining (Figure 2).

In 8.25 dpc wild-type embryos (Figure 2A), *Krox-20* is expressed in two broad domains of roughly similar size corresponding to the prospective r3 and r5 territories. At this stage, sharpening of the borders of expression is almost completed, but occasional *Krox-20*-expressing cells spread into even numbered territories (Figure 2A; Irving et al., 1996). In single and double mutants, both the spatial restriction and the size of pre-r3 and -r5 territories are normal (Figures 2B–2D). This normal *Krox-20* expression pattern in mutants was maintained through 9.0 dpc, when downregulation begins in r3 (Figures 2E–2H). Interestingly, at 9.0 dpc, abnormal folding of the dorsal lip of the r3 neuroepithelium was evident in single *Hoxa2*^{-/-} and, more prominently, in double mutants (Figures 2G and 2H, arrow).

Expression of *EphA4* in r3 and r5 also appeared normally restricted both in single and double homozygous mutants, with sharp boundaries from 8.25 to 10.5 dpc (Figures 2I and 2J; data not shown). In contrast, the *EphA4* r2-specific expression domain, normally appearing around 8.5 dpc (Irving et al., 1996), was absent both in *Hoxa2*^{-/-} and double mutants but normal in single *Hoxb2*^{-/-} mutants (Figure 2J; data not shown).

R4 segmentation also appeared normal. In both single and double mutant embryos, there was a normal sized r4 territory, inferred from the gap between r3 and r5 cells expressing *Krox-20* and *EphA4* (Figure 2). Furthermore, the r4 marker *Hoxb1* was expressed in this domain (data not shown). Thus, formation of r3 through r5 can occur independent of *Hoxa2* and *Hoxb2*.

Synergy between *Hoxa2* and *Hoxb2* in Patterning Interrhomomere Boundaries and Morphology

We next used *PLZF* as a marker to examine interrhomomere boundaries at 10.5 dpc in double mutants. At this stage, *PLZF* expression revealed a lack of clear boundaries between r1 and r4 (Figure 2L). Only the r4/r5 border was visible, although under Nomarski optics, a morphological boundary at the r5/r6 border was detected in flat-mount hindbrains. This was also confirmed by *Pax6* expression in the double mutants, which showed a lack of boundaries between r1 and r4 but not between r4 and more posterior segments (Figure 4F). It is noteworthy that expression of *EphA4* in r3 and *Pax6* in r4 were still segmentally restricted, even in the absence of r1 through r4 boundaries (Figures 2J and 4F).

The spatial distribution of *PLZF* in the r2–r3 region of double mutants was altered, resembling the normal r1 pattern: there was homogeneous ventrolateral staining,

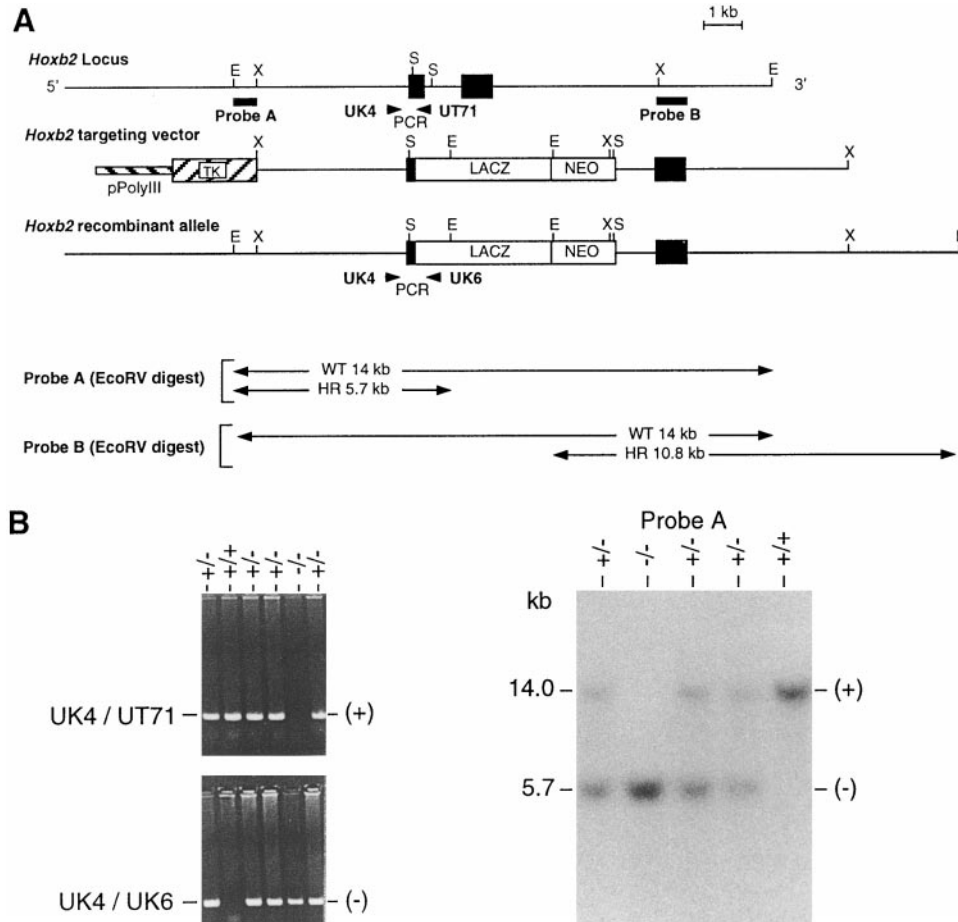


Figure 1. Targeted Disruption of the *Hoxb2* Locus

(A) *Hoxb2* wild-type locus, targeting vector, and *Hoxb2* mutant allele after homologous recombination (HR). The *LacZ/neo* cassette replaces most of *Hoxb2* exon 1 and contains two diagnostic *EcoRV* sites. Closed boxes represent exons. Primers used for PCR analysis (arrowheads) as well as the external probes (A and B) used for Southern analysis and the size of the expected hybridizing *EcoRV* genomic fragments are shown. Abbreviations: E, *EcoRV*; X, *XbaI*; and S, *Sall*.

(B) Genomic DNA genotype analysis by PCR and Southern blot (*EcoRV* digest and probe A). Wild-type (+) and mutant (-) allele bands are indicated. Primer combinations (PCR) and the size (kb) of each allele-specific band (Southern analysis) are shown. Corresponding genotypes at the *Hoxb2* locus are indicated above each lane.

and the dorsal column of low-*PLZF*-expressing cells normally extending from r2 to r6 was absent (Figure 2L). Moreover, the r1-r3 region was morphologically altered, since r1 appeared posteriorly extended at the expense of r2-r3 dorsal territories, showing a caudal shift of the pontine flexure (pf). Accordingly, there was a dorsolateral reduction of *EphA4* expression in r3 (Figure 2J). Overall, these abnormalities were more severe than those of single *Hoxa2*^{-/-} mutants (Gavalas et al., 1997), and in *Hoxb2*^{-/-} mutants, the interrhomomere boundaries appeared normal (data not shown). Thus, these results suggest functional synergy between *Hoxa2* and *Hoxb2* to generate correct rhombomere boundaries in the r2/r3 region.

Hoxa2 and *Hoxb2* Transcripts Display Specific D-V Distributions during Neurogenesis

In addition to their sharp A-P boundaries, some *Hox* genes display dynamic expression patterns along the D-V axis that correlate with events in neurogenesis (Graham et al., 1991). We analyzed *Hoxa2* and *Hoxb2* expression at 10.5 dpc along the D-V axis in the hindbrain

(Figure 3). For both genes, alternating regions of higher and lower expression were organized in broad longitudinal columns located at distinct D-V levels. They were expressed in similar dorsal columns, but in r3, *Hoxa2* displayed higher levels than *Hoxb2* (Figure 3, brackets). High levels of *Hoxb2* but not of *Hoxa2* were present in two ventral columns adjacent to the fp (Figure 3, arrowheads) that include progenitors and/or differentiating motor neurons. In r4, *Hoxa2*-expressing cells did not extend to the midline and appeared to abut the ventral columns of *Hoxb2* expression. Therefore, following early uniform expression, there is a columnar organization of *Hoxa2* and *Hoxb2* transcripts along the D-V axis at 10.5 dpc. These patterns define a set of complementary, partially overlapping, and quantitatively different distributions, strongly suggesting that *Hoxa2* and *Hoxb2* are linked to D-V patterning and neurogenesis.

Analysis of *Pax* Expression Reveals Defects in D-V Patterning

To investigate patterning along the D-V axis, we first analyzed *Pax3* and *Pax6* expression. At 10.5 dpc, *Pax3*

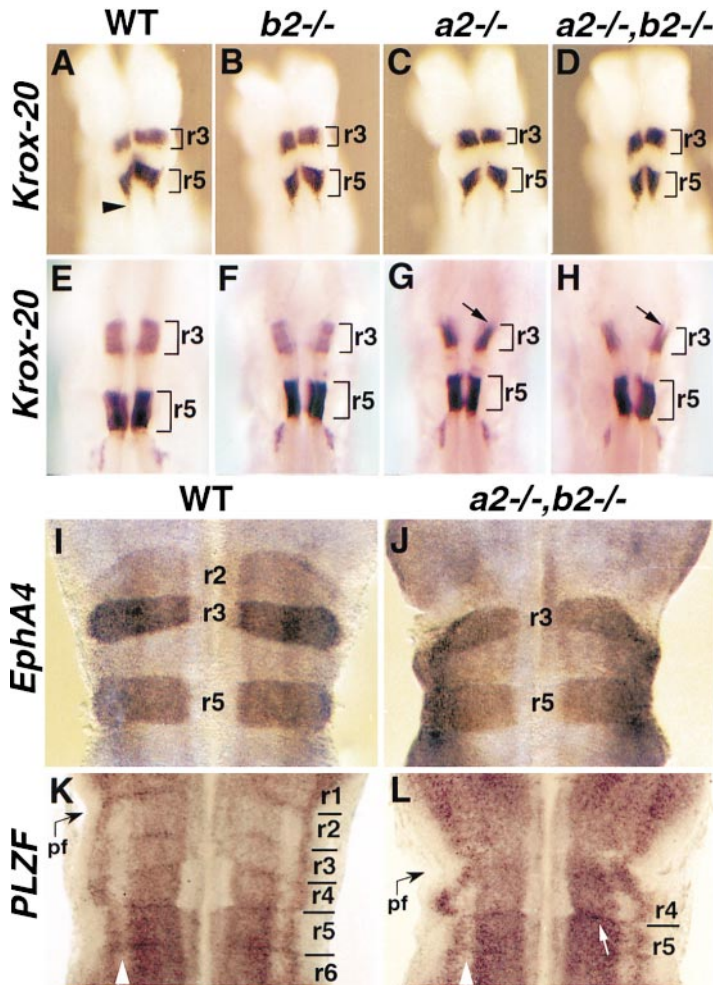


Figure 2. Normal Spatial Segregation of Rhombomeres in the Absence of Boundaries

(A–D) Dorsal views of 8.25 dpc wild type (A) and *Hoxb2*^{-/-} (B), *Hoxa2*^{-/-} (C), and double (D) mutants, stained with a *Krox-20* antibody, showing normal segregation of pre-r3 and pre-r5 *Krox-20*-expressing cells in the mutants. Normal *Krox-20* expression is also observed in neural crest cells migrating into the third branchial arch ([A], arrowhead).

(E–H) Dorsal views of 9.0 dpc wild type (E) and *Hoxb2*^{-/-} (F), *Hoxa2*^{-/-} (G), and double (H) mutants hybridized with a *Krox-20* antisense RNA. Normal restriction of *Krox-20*-expressing cells is observed in r3 and r5. Arrows in (G) and (H) indicate abnormal folding of the dorsal lip of the r3 neuroepithelium in *Hoxa2*^{-/-} and, more prominently, in double mutants, respectively.

(I and J) Dorsal views of flat-mounted wild-type (I) and double mutant (J) hindbrains at about 10.5 dpc hybridized with an *EphA4* antisense probe. Normal restriction of *EphA4* is observed in r3 and r5 of double mutants, with sharp expression boundaries, while the r2-specific expression domain is absent. Note also a dorsolateral reduction of *EphA4* expression in r3.

(K and L) Dorsal views of flat-mounted wild-type (K) and double mutant (L) hindbrains at 10.5 dpc hybridized with a *PLZF* antisense probe. In (L), only the r4/r5 border is clearly identifiable (white arrow). Note that the r1 territory appears to be posteriorly extended at the expense of r2–r3 dorsal territories, resulting in a caudal shift of the pf. The lateral distribution of *PLZF* transcripts in the r2–r3 region also appears altered, resembling the normal r1 pattern (arrowheads).

is normally expressed in a dorsal region throughout the rostrocaudal extent of the hindbrain neuroepithelium (Figure 4A; Goulding et al., 1993). In mutant hindbrains, *Pax3* expression was not significantly altered (Figures 4B and 4C). The main difference was a ventral shift in the border of *Pax3* expression toward the fp. In single *Hoxa2*^{-/-} and, more prominently, double mutants, there was a reduction in the number of ventral nonexpressing cells within the r2–r3 region (compare double headed arrows). This suggests abnormalities in the ventrolateral patterning of the r2–r3 region.

At 10.5 dpc, *Pax6* is expressed in dividing cells in a broad ventrolateral domain, excluding the fp and the adjacent region (Figure 4D). This domain partially overlaps with the ventral border of the *Pax3* expression domain, extending further ventrally (Goulding et al., 1993). *Pax6* labels two longitudinal columns, with higher expression levels in the r2–r6 region than in r1 (Figure 4D), suggesting that rhombomere-specific factors establish/maintain such differences. Rhombomere boundaries are weakly labeled, allowing easy identification of their position. In *Hoxb2*^{-/-} mutants, *Pax6* expression in the r1–r3 region was unchanged (data not shown). In contrast, *Pax6* expression was altered in both single *Hoxa2*^{-/-} and double mutants (Figures 4E and 4F). In *Hoxa2*^{-/-} mutants, *Pax6* was expressed at similar low levels

throughout the r1–r3 region, indicating downregulation in r2 and r3 (Figures 4D and 4E). The r1/r2 boundary was absent (see also Gavalas et al., 1997). Strikingly, in double mutants, there was an almost complete absence of *Pax6* expression in r3 (Figure 4F). Expression of the bHLH transcription factor *Mash1* (Figure 5C) revealed that *Pax6* downregulation in r2–r3 is not due to a massive loss of neuronal precursors.

These results indicate that *Hoxa2* is required to maintain high levels of *Pax6* expression in r2 and r3 and that in r3, the lack of *Hoxa2* can be partially compensated by *Hoxb2*.

Rhombomere-Specific Changes in Patterns of Neurogenesis

We next investigated the hindbrain distributions in single and double mutants of bHLH transcription factors, which have been shown to regulate distinct steps of neurogenesis (Kageyama and Nakanishi, 1997). We analyzed the expression of a mammalian *ac-sc* homolog, *Mash1*, which is expressed in subsets of neuronal precursors in both the CNS and peripheral nervous system (PNS) (Lo et al., 1991; Guillemot and Joyner, 1993; Ma et al., 1997). In the wild-type hindbrain, *Mash1* was expressed in broad longitudinal columns, subdividing the

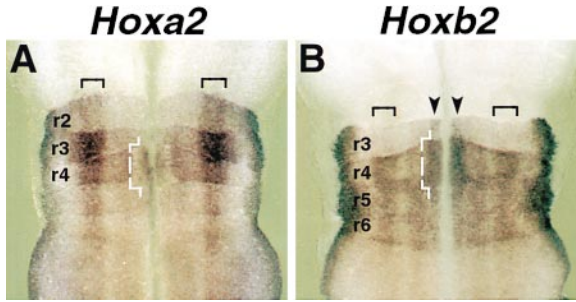


Figure 3. Specific D-V Expression of *Hoxa2* and *Hoxb2* during Neurogenesis

(A and B) Dorsal views of 10.5 dpc wild-type flat-mounted hindbrains hybridized with *Hoxa2* (A) and *Hoxb2* (B). Regions of higher and lower expression levels are organized in broad longitudinal columns at distinct dorsoventral positions. Both *Hoxa2* and *Hoxb2* are expressed in similar dorsal columns (black brackets), but in r3, *Hoxa2* displays higher expression levels. In contrast, in r4, higher *Hoxb2* levels are present in two ventral columns adjacent to the fp (arrowheads), whereas *Hoxa2* expression does not extend to the midline and abuts the ventral columns of *Hoxb2* expression (compare dashed lines).

ventricular zone into domains of expressing and non-expressing cells (Figure 5A). Interestingly, the *Mash1*-positive neuronal precursors displayed rhombomere-specific distribution. In r2–r5, *Mash1*-expressing cells segregated into three distinct columns on each side of the fp (Figure 5A, arrows). However, expression in the r1 ventral half was more homogeneous. In addition, the *Mash1* dorsal pattern in r4 was clearly distinct from that in r1–r3 and r5 (Figure 5A, bracket).

In *Hoxa2*^{-/-} hindbrains, a striking reorganization of *Mash1*-expressing cells was observed in the r2–r3 region, resembling the normal r1 pattern (Figure 5C). The r1-like distribution of *Mash1*-expressing cells displayed a sharp caudal limit at the r3/r4 border, whereas expression in r4 was apparently normal, and the hindbrain morphology rostral to r4 appeared as a caudally extended r1. In contrast, in *Hoxb2*^{-/-} mutants, specific alterations of *Mash1* expression were found in r4 but not in r2–r3 (Figure 5B). The r4 ventralmost column of

Mash1-expressing cells, just adjacent to the fp, appeared thinner than in wild type. It was reduced along its dorsal margin, resembling the column present in r2. In addition, *Mash1* expression appeared more homogeneous in the dorsal aspect of mutant r4 (Figure 5B, brackets).

We also examined the expression of the *atonal*-related gene *MATH-3* (Takebayashi et al., 1997). Its avian homolog, *NeuroM*, is expressed in postmitotic cells at the edge of the ventricular zone preceding migration to the outer layers (Roztocil et al., 1997). In wild-type flat-mounts at 10.5 dpc, *MATH-3* was expressed in two discrete ventral columns in r2 and r4 (Figure 5D), and these sites include the anlagen of the motor nuclei of the Vth and VIIth cranial nerves, respectively. The r4 column was thicker than in r2 and displayed a strong lateral and weak medial staining component. In *Hoxb2*^{-/-} mutants (Figure 5E), there was a reduction of the lateral aspect of the r4 column, now resembling the r2 column. These results, along with those of *Mash1*, raise the possibility that in *Hoxb2*^{-/-} mutants, there may be either a lack or an incorrect specification of a subset of ventral precursors, which may include VIIth nerve motor neuron precursors.

Next, we analyzed the expression of another *atonal*-related gene, *ngn2* (Gradwohl et al., 1996; Sommer et al., 1996) (Figures 5F–5I), which is also expressed in longitudinal columns of dividing precursors partially overlapping with the *Mash1* expression domains (Figures 5A and 5G). Dorsally, there was a stripe in r2 and more caudal rhombomeres (Figure 5G). Ventrally, *ngn2* expression was restricted to two columns (Figure 5G, arrows), with the more medial one displaying narrower and higher *ngn2* expression in r2–r5 than in r1. The adjacent *ngn2*-positive column was much thinner but also displayed higher expression levels in r2–r5 compared with r1. Interestingly, unlike *Mash1* and *MATH-3*, *ngn2* expression appeared to be largely excluded from ventral precursors (Figures 5A, 5D, and 5G). In r4, the ventral edge of this stripe displayed a characteristic indentation that appeared to frame the ventral expression domain of several motor neuron-specific markers, including *Nkx2.2*, *Phox2b*, *Hoxb1*, and *Isl1* (Figures 5G,

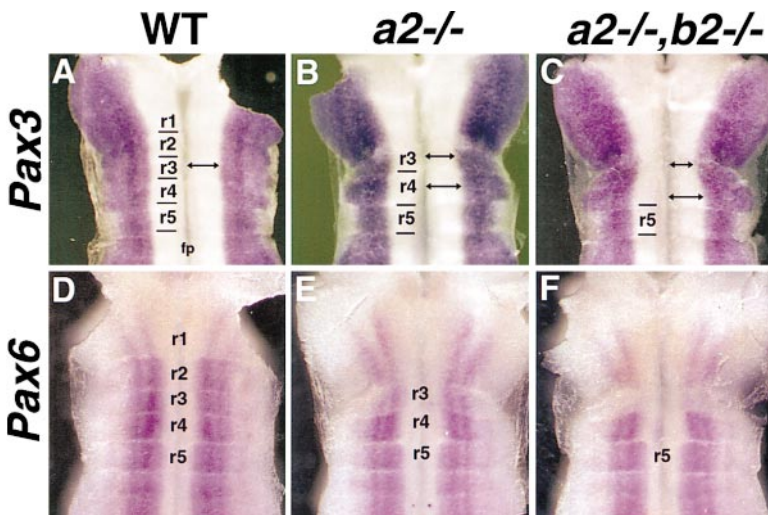


Figure 4. D-V Patterning Defects

(A–C) Dorsal views of flat-mounted 10.5 dpc wild type (A) and *Hoxa2*^{-/-} (B) and double (C) mutant hindbrains hybridized with a *Pax3* antisense probe. In (B) and, more prominently, (C), there is a medial (ventral) shift of the *Pax3* expression border toward the fp within the r2–r3 region compared with wild-type embryos or the immediately adjacent r4 region of the same mutants (compare double headed arrows in [A] through [C]).

(D–F) Dorsal views of 10.5 dpc flat-mounted wild type (D) and *Hoxa2*^{-/-} (E) and double (F) mutant hindbrains hybridized with a *Pax6* probe. In wild type (D), *Pax6* displays higher expression levels in r2–r6 than in r1. In single mutants (E), *Pax6* is expressed at similar low levels throughout the r1–r3 region, whereas in double homozygous mutants (F), there is an almost complete absence of *Pax6* expression in r3.

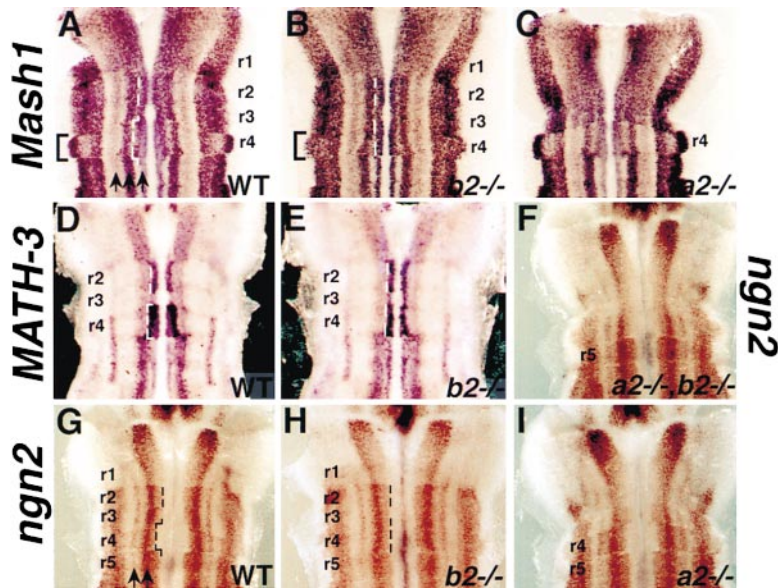


Figure 5. Rhombomere-Specific Alterations of bHLH Transcription Factors at 10.5 dpc
(A–C) Dorsal views of flat-mounted wild type (A) and *Hoxb2*^{-/-} (B) and *Hoxa2*^{-/-} (C) mutant hindbrains hybridized with a *Mash1* probe. In wild-type embryos (A), *Mash1* is expressed in broad longitudinal columns spanning the hindbrain length. *Mash1*-positive neuronal precursors display rhombomere-specific distribution patterns. In *Hoxa2*^{-/-} mutants (C), *Mash1*-positive cells in r2–r3 display a spatial distribution similar to that normally found in r1, with a sharp caudal limit at the r3/r4 border, as the r4 expression pattern is apparently normal. Rostral to r4, the morphology of the hindbrain appears as a caudally extended r1. In contrast, *Mash1* alterations are found in r4 but not in r2–r3 of *Hoxb2*^{-/-} mutants (B). The r4 ventralmost column of *Mash1*-expressing cells appears thinner than in wild type and resembles the r2 column (compare dashed lines). Furthermore, *Mash1* expression appears more homogeneous than in wild type in the dorsal aspect of r4 (brackets).
(D and E) Dorsal views of flat-mounted wild-type (D) and *Hoxb2*^{-/-} mutant (E) hindbrains

hybridized with a *MATH-3* probe. In wild type (D), *MATH-3* is expressed in longitudinal stripes, including two discrete ventral columns in r2 and r4 (dashed line) corresponding to the anlagen of the Vth and VIIIth nerve motor nuclei, respectively. The column in r4 is thicker than the one in r2 and displays a strong lateral staining component. In *Hoxb2*^{-/-} mutants (E), there is a reduction of the lateral component of the r4 column, now resembling the r2 column (dashed line).

(F–I) Dorsal views of flat-mounted wild type (G) and *Hoxb2*^{-/-} (H), *Hoxa2*^{-/-} (I), and *Hoxa2*^{-/-}/*Hoxb2*^{-/-} (F) mutant hindbrains hybridized with an *ngn2* probe. In wild type (G), *ngn2* is expressed in stripes of dividing precursors spanning the entire length of the hindbrain and partially overlapping the *Mash1* expression domains (compare [G] and [A]). In wild-type r4, there is a characteristic indentation at the edge of the ventralmost stripe, which is selectively lacking in *Hoxb2*^{-/-} mutants (compare dashed lines in [G] and [H]). In *Hoxa2*^{-/-} mutants (I), specific *ngn2* expression changes are found in the r2–r3 region, where *ngn2* levels appear reduced in the ventromedial stripe, becoming similar to those in r1, and in the two other more dorsal longitudinal stripes. In double mutants (F), *ngn2* expression in the r2–r3 region is further decreased.

6A, and 6C; data not shown). Interestingly, this *ngn2* pattern also parallels *Hoxa2* expression in the ventromedial part of r4 and its apparent exclusion from ventral motor neuron precursor columns (Figure 3A).

Specific changes in *ngn2* expression were found at 10.5 dpc in *Hoxa2*^{-/-} mutants (Figure 5I). In the r2–r3 territory, *ngn2* expression levels in the ventromedial column were reduced, approaching those in r1, and expression in the two other longitudinal stripes was downregulated although not abolished. In contrast, in *Hoxb2*^{-/-} mutants, *ngn2* expression in r2–r3 appeared normal (Figure 5H), but a subtle though consistent alteration was found ventrally in r4: the ventral margin of the inner column of *ngn2*-expressing cells did not show the specific indentation observed in wild type but appeared rather continuous with that of adjacent rhombomeres (dashed lines in Figures 5G and 5H). This implies that in the *Hoxb2*^{-/-} mutant r4, there has been a more ventral recruitment of *ngn2*-expressing precursors, similar to what normally occurs in r2. Analysis of *ngn2* expression in double mutant hindbrains (Figure 5F) revealed a further decrease of expression in the r2–r3 region as compared with single *Hoxa2*^{-/-} mutants (Figure 5I). This further supports synergistic interactions between *Hoxa2* and *Hoxb2* in regulating gene expression in the hindbrain.

Rhombomere-Specific and D-V Restricted Changes in Neuronal Patterning

We next analyzed three homeobox-containing genes that mark cells at precise D-V positions in the hindbrain

and are thought to control the identity of progenitor cells and/or aspects of neuronal differentiation—namely, *Nkx2.2* (Ericson et al., 1997), *Phox2b* (Pattyn et al., 1997), and *Evx1* (Burrill et al., 1997).

Nkx2.2 expression at 10.5 dpc is restricted to two stripes of ventral precursors, including presumptive motor neurons (Ericson et al., 1997), running on either side of the fp (Figure 6A). Similar to *Mash1* and *MATH-3*, the columns were thicker at the r4 level. In *Hoxa2*^{-/-} mutants, *Nkx2.2* displayed a normal distribution (data not shown). In contrast, in *Hoxb2*^{-/-} mutants, the *Nkx2.2* columns showed a dorsal reduction in r4 (Figure 6B).

Phox2b is expressed in both proliferating precursors and postmitotic neurons of specific classes, thus providing a possible link between early patterning events and the specification/differentiation of subsets of neuronal populations in the hindbrain (Pattyn et al., 1997). At 10.5 dpc, *Phox2b* is expressed in the wild-type hindbrain in two ventral columns (broader in r2 and even more so in r4) that include the developing Vth and VIIIth nerve motor nuclei, respectively (Figure 6C; Pattyn et al., 1997). In *Hoxb2*^{-/-} mutants (Figure 6D), clear reductions of the r4 ventral columns of *Phox2b*-expressing cells were observed, whereas the remainder of the expression pattern was apparently unchanged. Along with the results on *Nkx2.2*, *Mash1*, and *MATH-3* expression (Figures 5 and 6), this suggests an important role for *Hoxb2* in regulating a genetic cascade that may control the generation and/or fate of subsets of r4 motor neuron progenitors.

In contrast, in *Hoxa2*^{-/-} mutants, *Phox2b* expression was selectively lacking in the r2–r3 portion of the dorsal

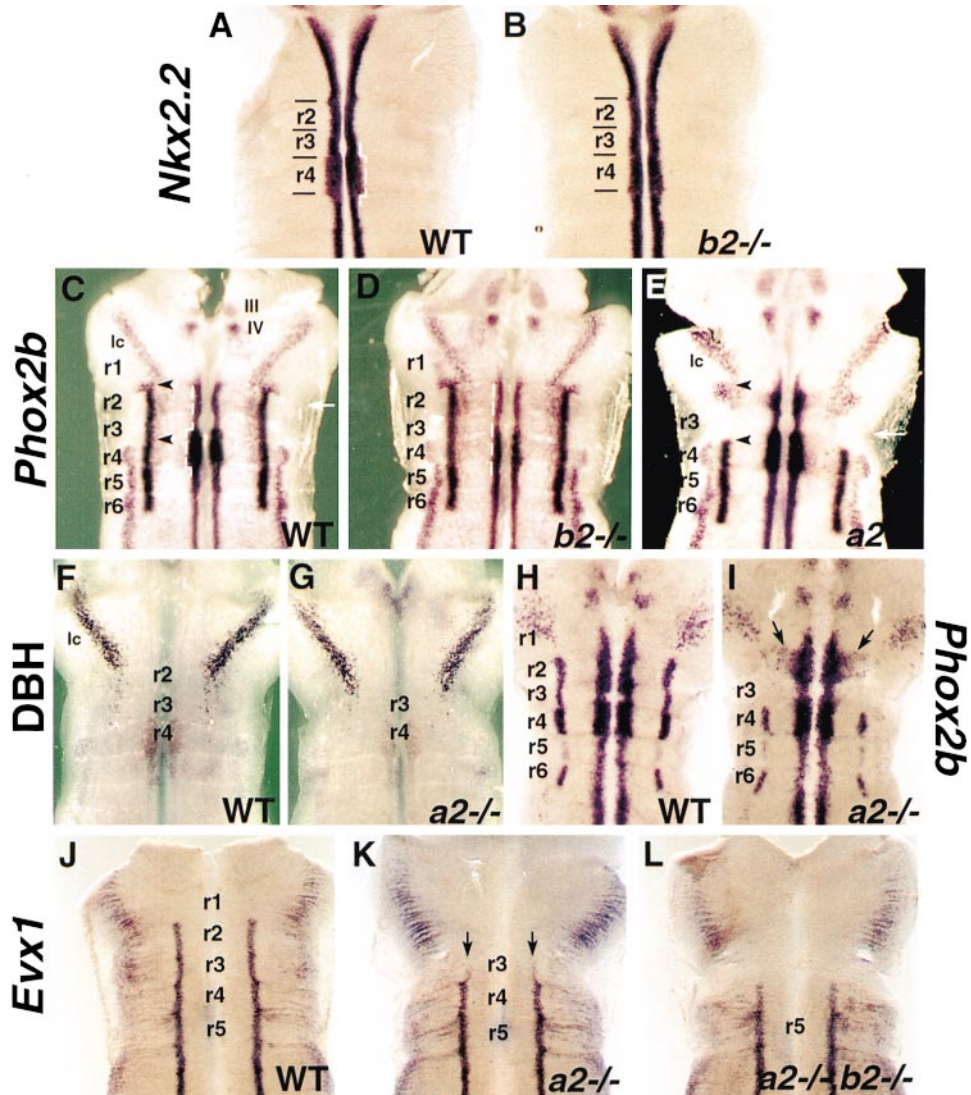


Figure 6. Rhombomere-Specific and D-V-Restricted Alterations of Homeobox Transcription Factors at 10.5 dpc

(A and B) Dorsal views of flat-mounted wild-type (A) and *Hoxb2*^{-/-} mutant (B) hindbrains hybridized with an *Nkx2.2* probe. In wild type (A), *Nkx2.2* expression is restricted to two stripes of dividing precursors adjacent to the fp. These stripes are thicker in r4. In *Hoxb2*^{-/-} mutants (B), a reduction of the dorsal (lateral) aspect of the r4 column is observed (compare dashed lines).

(C–E) Dorsal views of flat-mounted wild type (C) and *Hoxb2*^{-/-} (D) and *Hoxa2*^{-/-} (E) mutant hindbrains hybridized with a *Phox2b* probe. In wild type, (C), *Phox2b* is expressed in two ventral columns, broader in r2 and r4, containing the developing Vth and VIIIth nerve motor nuclei, respectively. Dorsally, another set of stripes extend from r2 to r6. *Phox2b* is also expressed in a stripe of differentiating neurons in the dorsal aspect of r1, representing the lc. In *Hoxb2*^{-/-} mutants (D), a reduction of the ventral column of *Phox2b*-expressing cells is observed in r4, now appearing as thick as in r2 (dashed line). In *Hoxa2*^{-/-} mutants (E), a selective lack of the r2–r3 portion of the lateral stripes is observed (arrowheads), while expression is still present ventrally, appearing even broader than in wild type. As the position of the pf is shifted posteriorly (compare white arrows), the r2–r3 ventral aspects appear included within a caudally extended r1 territory, suggesting mixed or nonhomogeneous segmental identities along the D-V axis. The r1-specific developing lc also appears to extend more caudally, with cells facing the r2 ventral column of *Phox2b*-expressing cells. This is confirmed by hybridization with the lc-specific marker DBH (F and G), suggesting that part of the r1 character has been extended posteriorly in *Hoxa2*^{-/-} mutants.

(H and I) Dorsal views of 9.25 dpc flat-mounted wild-type (H) and *Hoxa2*^{-/-} mutant (I) hindbrains hybridized with *Phox2b*. At this stage, expression is already lacking in the r2–r3 portion of the dorsal columns of mutants (I). The ventral r2 column is broader, and ectopic *Phox2b*-positive cells are found in more dorsolateral positions (arrows), indicating that ventral progenitor cells are being generated in ectopic locations and/or early differentiating neurons are prematurely migrating to more lateral positions.

(J–L) Dorsal views of 10.5 dpc flat-mounted wild type (J) and *Hoxa2*^{-/-} (K) and double (L) mutant hindbrains hybridized with *Evx1*. In wild type (J), *Evx1* is expressed in two stripes of ventral interneurons, with a sharp anterior limit at the r1/r2 border. In *Hoxa2*^{-/-} mutants, expression is selectively lacking in r2 and partially lacking in r3 (arrows). In double mutants (L), expression in r3 is completely abolished. III and IV, oculomotor and trochlear motor nuclei, respectively.

columns normally extending from r2 to r6 (Figure 6E, arrowheads). Such domain of expression was already absent at 9.25 dpc (Figure 6I), suggesting that *Hoxa2*

may activate *Phox2b* dorsally in r2–r3. The position of the pf was shifted posteriorly (Figure 6E, arrow), and the locus coeruleus (lc), normally in the dorsal aspect of r1,

also appeared to extend more caudally (Figure 6E). This was confirmed by dopamine- β -hydroxylase (DBH) gene expression as an lc-specific marker (Figures 6F and 6G). These results suggest that part of the r1 character has been extended posteriorly. However, there was no corresponding lack of r2–r3 expression in the most ventral columns of *Phox2b* expression, which included the developing Vth cranial nerve motor nuclei (Pattyn et al., 1997). Instead, at both 9.25 and 10.5 dpc expression was actually stronger and broader in the r2 ventral columns (Figures 6E and 6I). At 9.25 dpc, *Phox2b*-expressing cells were found in more dorsal positions (Figure 6I, arrows), indicating that ventral progenitors and/or early differentiating neurons were being generated in ectopic locations or were prematurely migrating dorsally. Thus, included within the caudally extended r1 territory were *Phox2b* expression patterns resembling those normally found in the ventral aspects of r2 and r3. This suggests that mixed or nonhomogeneous segmental identities arise in *Hoxa2*^{-/-} mutants along the D-V axis.

Evx1 is expressed in specific ventral interneurons soon after these cells cease mitosis (Burrill et al., 1997). In the wild-type hindbrain at 10.5 dpc, *Evx1* was expressed in two thin stripes, with sharp anterior limits at the r1/r2 border running in a ventrolateral region included within the *Pax6* expression domain (compare Figures 4D and 6J). No changes in *Evx1* expression were found in *Hoxb2*^{-/-} mutants (data not shown). In contrast, we observed a specific lack of *Evx1* expression in r2 and, partially, r3 of *Hoxa2*^{-/-} mutants (Figure 6K, arrows). This residual *Evx1* expression in r3 was abolished in double mutants (Figure 6L).

Altered D-V Neuronal Differentiation Patterns in *Hoxa2*^{-/-} Mutant Hindbrain

To examine neuronal differentiation patterns in wild-type and *Hoxa2*^{-/-} mutants, we used two neurofilament probes. An RNA probe (NF-M) probe mainly labels cell bodies of early differentiating neurons, including motor neurons and reticular and alar plate neurons, while a 2H3 anti-neurofilament antibody marks both cell bodies and axons (Figures 7A and 7C). In the hindbrain, neurogenesis follows a temporal sequence, with neurons differentiating first in even rhombomeres (Lumsden and Keynes, 1989). Accordingly, in wild type at 22–25 somites, motor neuron differentiation in r2 and r4 was more advanced than in odd rhombomeres (Figures 7A and 7C). Motor neuron cell bodies formed discrete longitudinal columns on either side of the fp and projected axons dorsally (laterally) toward the exit points of the Vth and VIIIth cranial nerves. However, in *Hoxa2*^{-/-} mutants, motor neuron cell bodies in r2 were not clearly organized in discrete ventral columns (Figures 7B and 7D). Overall, D-V neuronal distribution was abnormal, with cell bodies in more dorsal positions, suggesting ectopic neurogenesis or premature migration of motor neurons. Moreover, while in wild type, the r2 exit points displayed a one rhombomere width, the mutant r2 exit points were strongly reduced along the rostrocaudal axis, as seen by the converging trajectories of motor axons (Figures 7C and 7D, brackets). Furthermore, in wild-type r3, a group of neurons was labeled in the alar plate (Figure 7A, bracket), overlapping the lateral longitudinal tracts

(II), but in mutants, staining in the alar plate was lacking between the exit points (Figure 7B).

The 2H3 antibody also labeled the II (Clarke and Lumsden, 1993), composed of descending tectobulbar and tectospinal axons, ascending and descending axons from hindbrain, and sensory neuron axons ingressing from the periphery (Figure 7C). In *Hoxa2*^{-/-} mutants, alterations were found in II pathfinding in the r2–r3 region (Figure 7D, arrowheads). Numerous axon fascicles abruptly terminated at the level of the r2 exit point and did not run through the alar plate in r3. The few axon fascicles in alar r3 appeared to avoid the most lateral region and converged at the r2 exit point. In the r2–r3 region, the most lateral axons are the facial and vestibulo-acoustic sensory axons ingressing r4 and running rostrally, as well as the trigeminal afferents ingressing r2 and running caudally (Clarke and Lumsden, 1993). We used retrograde dye labeling at 10.5 dpc to investigate the Vth and VIIIth ganglion sensory neuron projections in *Hoxa2*^{-/-} mutants (Figures 7E and 7F). In wild-type embryos, 3,3'-diiodoacetyl-5,6-diamino-2,4,6-tetramethylindocarbocyanine perchlorate (Dil; red) injections at the Vth and VIIIth cranial nerve ganglia, respectively, labeled the central processes of ascending and descending sensory axons and their entry point regions, as well as motor neuron axons and their exit points (Figure 7E; Clarke and Lumsden, 1993). In mutants, there was a selective lack of the ascending processes of facial and vestibulo-acoustic sensory axons ingressing from r4 into the r3 alar plate (Figure 7F). Descending processes were present but slightly reduced in number. At the r2 level, both the trigeminal sensory axon entry point (SEP) and the motor neuron exit point (MEP) regions were reduced (Figures 7E and 7F), in agreement with the 2H3 antibody staining (Figure 7D). Altered motor axon pathfinding in the r2–r3 region was also evident in the mutants (Figure 7F; Gavalas et al., 1997).

Together, these results revealed changes in the D-V distribution and differentiation patterns of early neurons in *Hoxa2*^{-/-} mutants restricted to the ventrolateral and alar plate regions of r2–r3.

Facial Nerve Motor Nucleus Defects in *Hoxb2*^{-/-} Mutants

The marked downregulation of motor neuron markers (*Nkx2.2*, *Phox2b*, *Isl1*) in r4 ventral columns of *Hoxb2*^{-/-} mutants at 10.5 dpc (Figure 6; data not shown) suggested impairment of facial motor nucleus development. To address this point, we performed Dil labeling at 10.5 dpc. Dil injections at the facial nerve exit point of wild-type embryos labeled r4 and r5 motor neurons (Figure 7G). At this stage, r4 branchiomotor neurons that will form the somatic motor component of the facial nerve are migrating caudally into r5 (Auclair et al., 1996; Studer et al., 1996; McKay et al., 1997). In *Hoxb2*^{-/-} mutants, the number of such migrating neurons appeared greatly reduced in r5 (Figure 7H, arrows). In addition, a few laterally migrating r3 neurons incorrectly projected to the r4 exit point (Figure 7H, arrowhead), similar to *Hoxa2*^{-/-} mutants. Anti-ISL1 antibody staining at 13.5 dpc confirmed a severe reduction but not absence of the facial motor nucleus in five out of five *Hoxb2*^{-/-} mutants analyzed (data not shown).

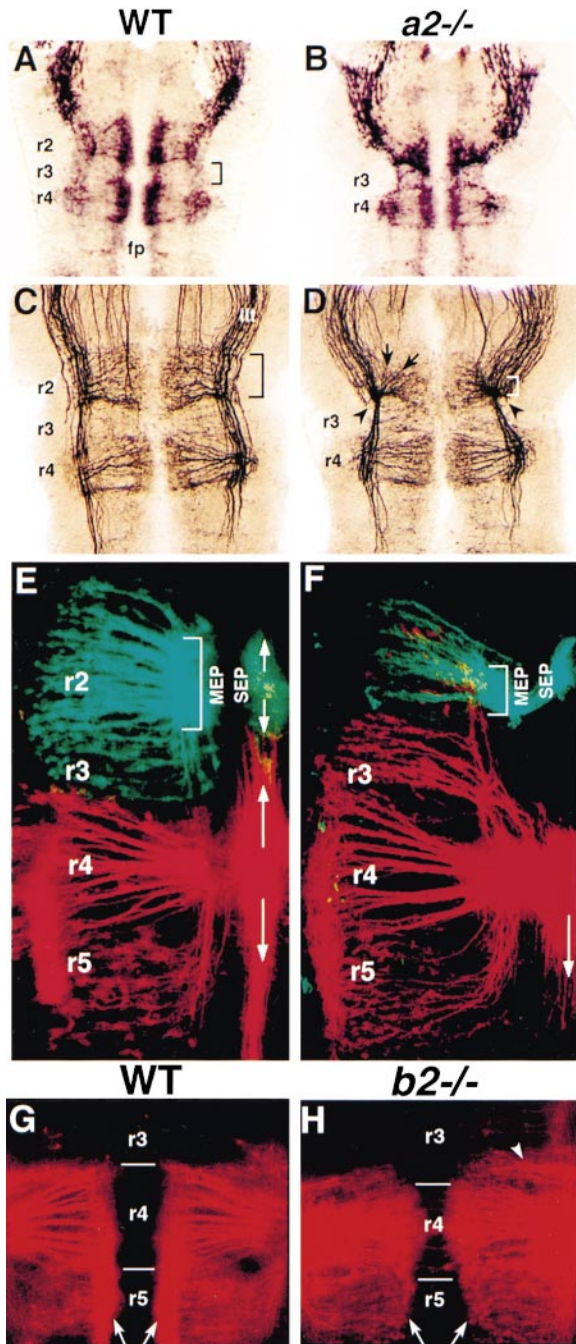


Figure 7. Altered D-V Neuronal Differentiation Patterns and Impaired Facial Motor Nucleus Development

(A–D) Dorsal views of 9.25 dpc (22–25 somites) flat-mounted wild-type (A and C) and *Hoxa2*^{-/-} mutant (B and D) hindbrains stained with a neurofilament riboprobe (A and B) and the 2H3 anti-neurofilament antibody (C and D).

(A) In wild type, r2 and r4 motor neurons form discrete columns on either side of the fp, and project their axons (C) dorsally (laterally) toward the exit points of the Vth and VIIIth cranial nerves, respectively. In r3, a group of neurons is labeled in the alar plate (bracket in [A]), which overlaps with the lateral Ilt in (C).

(B and D) In *Hoxa2*^{-/-} mutants, r2 motor neuron cell bodies are not clearly organized in discrete ventral columns; in addition, overall D-V neuronal distribution is abnormal (arrows). The r2 exit points in mutants are strongly reduced, as seen by the converging trajectories of motor axons (brackets in [D]). Furthermore, a lack of staining is

This analysis thus confirms that the development of the somatic motor component of the facial nerve is impaired in *Hoxb2*^{-/-} mutants, reminiscent of the phenotype described for *Hoxb1* mutants (Goddard et al., 1996; Studer et al., 1996).

Discussion

We examined *Hoxa2* and *Hoxb2* functions in hindbrain patterning. Single and double mutant analysis showed that the normal number of segments form, but boundaries between r1 and r4 are incorrectly generated at later stages, suggesting changes in rhombomere segmental identities. We focused on rhombomere-specific changes in neurogenesis by examining expression of transcription factors controlling the fate and differentiation of neuronal precursors (Figure 8). We find that *Hoxa2* and *Hoxb2* are coupled to both A-P and D-V patterning and identify genetic cascades linking *Hox*-mediated patterning to neurogenesis in the developing hindbrain. These observations correlate with *Hoxa2* and *Hoxb2* transcripts being differentially distributed along the D-V axis in columnar domains during neurogenesis and raise a number of interesting issues.

Hoxa2 and *Hoxb2* Are Not Required for r3–r5 Segmental Generation

Krox-20 inactivation resulted in the loss of r3 and r5 by 10.0 dpc (Schneider-Maunoury et al., 1997). Since *Hoxa2* and *Hoxb2* are direct targets of *Krox-20* in r3 and r5 (Sham et al., 1993; Nonchev et al., 1996), the *Krox-20* mutant phenotype could result from deregulation of these genes. However, analysis of *Krox-20* and *EphA4* expression clearly identifies r3 and r5 territories in double mutants (Figure 2). Moreover, at late stages, the distance between the facial and trigeminal nuclei was

observed in the r3 alar plate between the exit points (B). Antibody staining in the r2–r3 region shows alterations in the Ilt pathfinding (D); numerous axon fascicles abruptly terminate at the level of the r2 exit point (arrowheads) and do not run through the r3 alar plate. Fewer axons are present in alar r3; they appear to avoid the most lateral region and converge at the r2 exit point.

(E and F) Retrograde DiO (green) and Dil (red) labeling at 10.5 dpc of the Vth and VIIIth cranial nerves, respectively, in wild-type (E) and *Hoxa2*^{-/-} (F) embryos.

(E) In wild type, DiO (green) and Dil (red) injections label the central processes of ascending and descending sensory axons (arrows) of the Vth and VIIIth/VIIIth nerves, respectively, and their entry point regions as well as motor neuron axons and their exit points.

(F) In mutants, the ascending processes of facial and vestibulo-acoustic sensory axons, ingressing from r4, are not labeled in alar r3. In r2, both the trigeminal SEP and MEP (bracket) regions are reduced, consistent with the antibody staining at 9.25 dpc in (D). r2 and r3 motor axon pathfinding defects in the r2–r3 region are also evident (Gavalas et al., 1997).

(G and H) Dorsal views of flat-mounted 10.5 dpc wild-type (G) and *Hoxb2*^{-/-} mutant (H) hindbrains after retrograde Dil tracing of r4 and r5 motor neurons. In wild type (G), Dil injections at the facial nerve exit point labels motor neurons and their axons in r4 and r5. At this stage, the cell bodies of r4 facial branchiomotor neurons are migrating caudally into r5 (arrows). In mutants (H), the number of such migrating neurons appears greatly diminished in r5 (arrows). Moreover, a few laterally migrating r3 motor neurons incorrectly project to the r4 exit point (arrowhead).

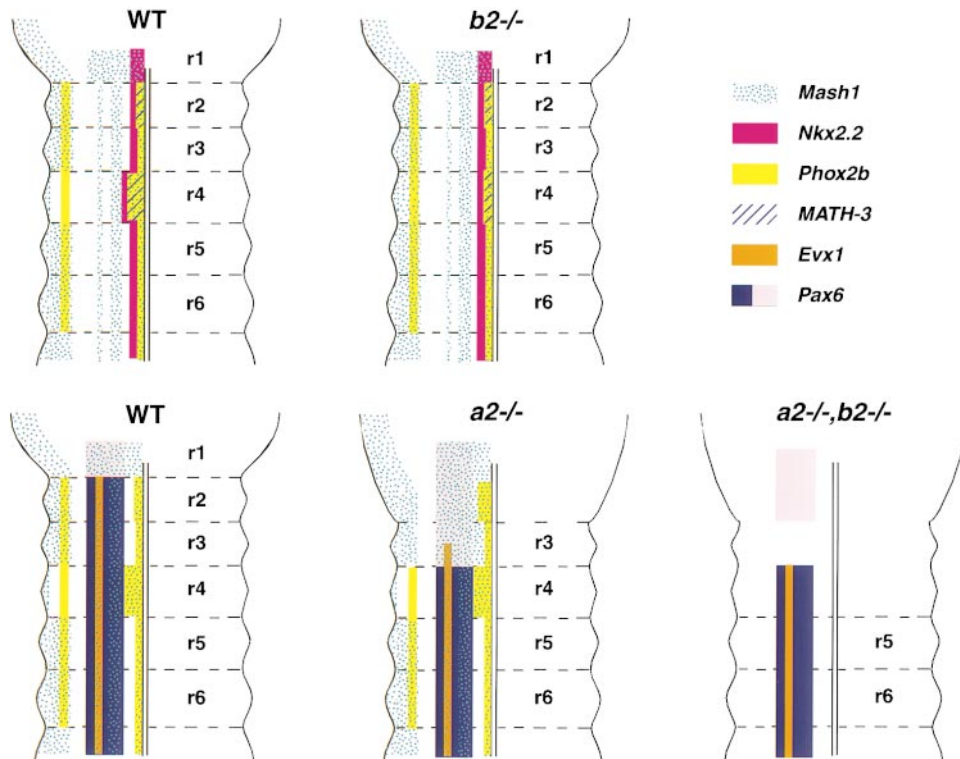


Figure 8. Summary of the A-P and D-V Molecular Changes Observed in Single and Double Mutant Hindbrains

Schematic representation of the most relevant expression changes of the molecular markers described for each mutant. Changes in hindbrain morphology are also indicated. For *MATH-3* and *Phox2b*, we only show the subset(s) of their expression patterns that is relevant to the observed changes. In the double mutant panel, we have indicated only those genes, namely *Pax6* and *Evx1*, whose expression patterns display alterations not already seen in single mutants. The superimposition of transcript distributions, to show their relative spatial relationships, is based on double whole-mount in situ hybridizations (data not shown). *Pax3*, *ngn2*, neurofilament, and DBH expression patterns have not been indicated for simplicity.

not as reduced, and Vth and VIIth nerve sensory ganglia were not fused (data not shown), both hallmarks of segmental defects in *Krox-20* null mutants. Thus, the generation and maintenance of rhombomeric territories occurs normally in double mutants. Therefore, the loss of r3 and r5 in *Krox-20* mutants must be mediated through different downstream targets.

Functional Synergism between *Hoxa2* and *Hoxb2* in Interrhombomere Boundary Formation

While *Hoxb2* inactivation did not appear to alter boundary formation, the r1/r2 and r2/r3 boundaries were absent and partially affected in *Hoxa2*^{-/-} mutants, respectively (Gavalas et al., 1997). Functional synergy between *Hoxa2* and *Hoxb2* is evident, as the double mutant phenotype is more severe than that of *Hoxa2*^{-/-} mutants. Segmentation involves repulsive *Eph/ephrin*-mediated interactions between adjacent segments (Xu et al., 1995), leading to the progressive establishment of differential adhesive properties (Wizenmann and Lumsden, 1997). These processes restrict cell mixing between adjacent segments and are followed by the transient appearance of overt morphological boundaries at the interfaces between odd and even rhombomeres (e.g., Guthrie and Lumsden, 1991), constraining the position

and differentiation of groups of cells along the main axis. Mutations in *Hoxa2* and *Hoxb2* appear to result in changes of regional identity associated with lack of borders in the rostral hindbrain, suggesting that generation and maintenance of segmental identity is important in establishing interrhomomere boundaries. The maintenance of properly restricted *EphA4* expression in double mutants (Figure 2) is consistent with the idea that it is independently regulated by other factors, such as *Krox-20* (Theil et al., 1998). Since the *EphA4* expression is restricted to sharp domains at a time when *PLZF* expression in r1 through r4 rhombomere boundaries is missing, this strongly suggests that separate mechanisms are associated with cell-cell recognition and sorting compared with the formation of rhombomere boundaries. These findings are also in line with analysis in the hindbrains of mouse and fish *kreisler/valentino* mutants, which show that it is possible to have sharp segmentally restricted patterns of gene expression in the absence of boundary formation in the caudal hindbrain.

While there is normal r3 and r5 *EphA4* expression in the mutants, this does not help us to formally distinguish whether the degree of cell mixing has been changed. This would require time-lapsing of single labeled cells in vivo. However, we note that if there were increased

cell mixing between r3 (r5) and adjacent territories, a high degree of regulation of gene expression would be required to keep *EphA4* expression segmentally restricted and with sharp boundaries.

Analysis of *Pax* Expression Reveals Defects in D-V Patterning

Several *Pax* genes, including *Pax3* and *Pax6*, are expressed in D-V restricted domains of the developing spinal cord and hindbrain in neural progenitors during early neurogenesis (Goulding et al., 1993). Establishment of such D-V restricted expression domains is regulated by the inductive actions of *Shh* and bone morphogenetic proteins (BMPs) (Tanabe and Jessell, 1996; Ericson et al., 1997). Mutant studies have shown that *Pax3* and *Pax6* are important determinants of dorsal and ventral differentiation pathways of neural progenitors, respectively (Stuart et al., 1994; Ericson et al., 1997; Osumi et al., 1997).

In the rostral hindbrain, assignment of D-V positional values is still labile at the time when A-P positional information has already been fixed (Simon et al., 1995). We have shown that in the absence of *Hox* patterning information, D-V patterning is also affected. In single and double mutants, we found alterations in the D-V restriction of the *Pax3* domain and in the levels of *Pax6* selectively in r2 and r3, where *Hoxa2* and *Hoxb2* are the only *Hox* genes expressed. *Pax3* dorsal restriction and the sharpening of its ventral boundary are the result of *Shh*-mediated repression in the ventral neural tube (Tanabe and Jessell, 1996). High *Shh* concentrations also repress *Pax6* in ventral progenitors adjacent to the fp, allowing concomitant activation of ventral markers (Ericson et al., 1997). The altered *Pax3* and *Pax6* expression observed in *Hoxa2*^{-/-} and double mutants (Figure 4) may thus reflect an impairment in perceiving the *Shh* signal by ventral cells or in maintaining stable states of activated/repressed *Pax* gene expression in response to such signals. Another possibility is that *Shh* is regulated by *Hox* genes. However, we exclude such a possibility, as mutant analysis shows no changes in *Shh* expression (data not shown). Downregulation but not absence of *Pax6* in r2 and r3 of *Hoxa2*^{-/-} mutants indicates that *Hoxa2* is required, directly or indirectly, to maintain high levels of *Pax6*. The additional lack of *Hoxb2* in r3 results in a more severe impairment in *Pax6* expression, supporting a role for *Hox* paralog group 2 genes in the maintenance of *Pax6*. This implies that populations of dividing neural progenitors in the rostral hindbrain might continuously reassess their A-P positional values in order to maintain correct D-V specification.

It has been shown that dorsal expansion of ventral markers occurs in the caudal hindbrain and spinal cord of *Pax6* mutant *Sey/Sey* mice (Ericson et al., 1997). Lower *Pax6* levels in our mutants may thus result in derepression of some ventral progenitor markers whose expression may expand in the territory normally occupied by *Pax6*. In this respect, it is noteworthy that the ventral expression domains of *Phox2b* extended to slightly more dorsal positions in *Hoxa2*^{-/-} mutant r2 (Figure 6l). In addition, r2 motor neurons may be located in slightly more dorsal positions than in wild type already at an early developmental stage (Figures 7A–7D).

Finally, *Pax6* downregulation may also affect progenitor dispersal in the ventral neural tube at r2–r3 levels. In *Hoxa2*^{-/-} and double mutants, ventral progenitor movements may not be properly restricted, resulting in altered spatial domains of the above markers. In this respect, it is noteworthy that first, dispersal of neuroepithelial cells in the wild-type hindbrain is not uniform but is related to position along the D-V axis (Clarke et al., 1998), and second, adhesive properties of cells are altered in the developing CNS of *Sey/Sey* mice, leading to segregation defects (Stoykova et al., 1997).

Differential Regulation of Genes Involved in Neurogenesis and Specification of Progenitor Cell Fate

In the developing neural tube, multipotent progenitor cells may acquire their specific fate according to their position on a grid of Cartesian coordinates (Wolpert, 1969) established at the intersection of signaling centers acting along both the A-P and D-V axes (Ye et al., 1998). Accumulating evidence indicates that secreting tissues and signaling molecules instructing cell fate along the A-P and D-V axes also affect expression of *Hox* and *Pax* genes, respectively (Itasaki et al., 1996; Lumsden and Krumlauf, 1996; Tanabe and Jessell, 1996; Ericson et al., 1997; Grapin-Botton et al., 1997; Ensini et al., 1998; Gould et al., 1998). In addition, knockout experiments strongly suggest the involvement of *Hox* and *Pax* genes in the specification of neuronal identity (Goddard et al., 1996; Studer et al., 1996; Ericson et al., 1997; Osumi et al., 1997; Tiret et al., 1998), indicating that these gene products may be the functional readout of such signals. Here, we show that *Hox*-encoded positional information and neurogenic programs are integrated in progenitor cells to specify distinct neuronal fates.

One potential link is that signals operating on A-P and D-V axes induce patterning genes, such as *Hox* and *Pax*, which in turn define restricted expression domains of genes controlling neurogenesis and progenitor cell fate. In relation to the alterations in *Pax* expression observed in single *Hoxa2*^{-/-} and double mutants, it is relevant that the lack of *Pax6* function in *Sey/Sey* mice resulted in changes in progenitor cell identity, leading to abnormal specification of motor neurons and ventral interneurons in the spinal cord and caudal hindbrain (Burrill et al., 1997; Ericson et al., 1997; Osumi et al., 1997), therefore strongly suggesting cell identity changes in *Hox* paralog group 2 gene mutants as well. Such changes may also be associated with differences in the proliferative properties of precursor cells. Moreover, the almost lack of *Pax6* expression in r3 of double mutants, while low expression levels remain in the r1–r2 region, suggests that such alterations cannot simply result from changes in the rostrocaudal identities of precursors.

To gain insights into the genetic cascade regulating neuronal cell fate downstream of *Hoxa2* and *Hoxb2*, we analyzed the spatial distributions of several transcription factors normally expressed in dorsoventrally restricted longitudinal columns of neuronal progenitors (*Mash1*, *ngn2*, *Phox2b*, *Nkx2.2*) and immature neurons (*MATH-3*) (Figures 5, 6, and 8). In addition, we investigated neuronal differentiation both at the cellular level (retrograde dye labeling and antineurofilament antibody staining;

Figure 7) and by means of molecular markers of differentiating neuronal subtypes (*Evx1*, *Phox2b*, DBH, *Isl1*; Figures 6 and 8; data not shown). Rhombomere-specific alterations in the columnar arrays of neuronal precursors expressing the above markers were observed in each mutant, which correlated with altered neuronal cell patterns.

Two interesting conclusions arise from these findings. First, expression of a given molecular marker (*Mash1*, *ngn2*, *Phox2b*) in longitudinal stripes of neuronal precursors running the length of several rhombomeres displays a "modular" regulation, as it is differentially controlled by *Hoxa2* or *Hoxb2* in specific segments. While *Hoxa2* appears to control the distribution of subsets of neuronal precursors in r2 and r3, *Hoxb2* exerts its function mainly in r4. As several nuclei of the mature hindbrain display a plurisegmental origin (Marin and Puelles, 1995), these results raise the possibility that *Hoxa2* and *Hoxb2* could be involved in ensuring the fidelity of the patterning of some of these structures by defining segment-specific, spatially restricted arrays of progenitor cell deployment along the A-P axis. In addition, these data further support the hypothesis of alterations in progenitor identity in the mutants, since, for example, both *Mash1* and *ngn2* have been implicated in the regulation of specific neuronal phenotypes (Fode et al., 1998; Hirsch et al., 1998; Lo et al., 1998).

Second, in a given segment, *Hoxa2* or *Hoxb2* appears to regulate only subsets of the expression patterns of downstream genes (*Mash1*, *ngn2*, *Phox2b*), consistent with the idea that their function may be restricted along the D-V axis. Morphological and cellular analyses of single mutants support the idea that *Hoxa2* controls development in the alar and "dorsal" basal plates of r2 and r3, whereas *Hoxb2* is essential for motor neuron development in the "ventral" basal plate of r4. Alterations of molecular and cellular markers are found in the mutants in those regions of the neuroepithelium where *Hoxa2* or *Hoxb2* normally displays the highest relative expression levels along the D-V axis at 10.5 dpc (Figures 3A and 3B). Thus, *Hoxa2* and *Hoxb2* might be involved in the maintenance of rhombomere-specific gene expression, marking distinct, D-V restricted, neuroepithelial cell populations in r2-r3 and r4, respectively. In addition, *Hoxa2* and *Hoxb2* can functionally synergize in r3, as suggested by the complete lack of expression of *Evx1*, a marker for a ventral interneuron subtype (Burrill et al., 1997), in double but not in single mutants (Figures 6J-6L). This latter finding may directly relate to the synergistic alterations in *Pax6*, *Mash1*, and *ngn2* expression observed in r3 ventral neuronal progenitors of double mutants, suggesting that *Evx1* may be further downstream in a genetic cascade regulated by *Hoxa2* and *Hoxb2*, controlling the specification of ventral progenitor cell fate in r3. These results do not rule out the possibility that *Hoxa2* and/or *Hoxb2* may be directly involved in the establishment of early expression patterns. For example, we show that the r2-r3 portion of the *Phox2b*-expressing dorsal column is already lacking at 9.25 dpc in *Hoxa2*^{-/-} mutants (Figure 6I), suggesting that *Phox2b* early activation is dependent on *Hoxa2* in that region and therefore raising the possibility of *Phox2b* being a direct *Hoxa2* target.

In conclusion, our results may provide insights into the

mechanisms that generate precise patterns of discrete neuronal cell types within specific rhombomeres. Since in the hindbrain, cells may be restricted early in their fate (Lumsden et al., 1994) due to the limited dispersal of precursors along both the A-P and the D-V axes (Fraser et al., 1990; Clarke et al., 1998), the understanding of how the expression of genes controlling neurogenesis and progenitor fate is spatially regulated provides a direct way to learn how cell fates are assigned at reproducible positions within a given segment.

Facial Branchiomotor Neuron Specification and *Hoxb2* Function

Our data confirmed those of a previous report (Barrow and Capecchi, 1996) implicating *Hoxb2* in the development of the facial nerve motor nucleus and possibly suggesting its genetic interaction with *Hoxb1*. In contrast to those mice in which *Hoxb1* regulation is affected in *cis*, in our *Hoxb2*^{-/-} mutants, *Hoxb1* expression in r4 was not abolished (data not shown). However, the facial motor nucleus phenotype of homozygous mutants was reminiscent of that described in *Hoxb1*^{-/-} mutants (Goddard et al., 1996; Studer et al., 1996), indicating that both *Hoxb2* and *Hoxb1* are required for facial nerve development. *Hoxb1* may be exerting its influence primarily through *Hoxb2*, as we have shown that *Hoxb2* is a direct target of *Hoxb1* in the hindbrain (Maconochie et al., 1997). Retrograde Dil labeling of *Hoxb2*^{-/-} mutants at 10.5 dpc indicated a paucity of r4 branchiomotor neurons migrating into r5 (Figure 7). This suggests either (1) an alteration of the migratory properties of r4 branchiomotor neurons, (2) a lack of generation of r4 branchiomotor neuron progenitors, or (3) a possible change of r4 progenitor cell fate. Interestingly, we found consistent "dorsal" reductions of the ventral columns of r4 expression of several molecular markers expressed, at 10.5 dpc, in early differentiating motor neurons or proliferating progenitors (Figures 5 and 6). Altogether, these data strongly support the possibility of developmental alterations of the facial branchiomotor progenitor pool in mutants. Moreover, the dorsal reduction in mutant r4 of the ventral columns of expression of the above motor neuron-specific markers (Figures 5 and 6) may correlate with the ventral expansion of the *ngn2* expression domain (Figure 5H). This latter finding may indirectly support the hypothesis of cell fate changes rather than depletions in the progenitor pool. Detailed cellular studies will be required to provide direct evidence for such an hypothesis.

Thus, in addition to uncovering the requirement of *Hoxb2* and its interaction with *Hoxa2* for normal r3 patterning, our study provides insights into the genetic cascade that may control the generation/specification of r4 branchiomotor neurons downstream of *Hoxb2*.

Conclusion

Little is known about the mechanisms integrating A-P and D-V positional information with the neurogenic programs that enable the generation of distinct neuronal types at stereotypic positions within the developing neural tube. Here, we show that during neurogenesis, *Hoxa2* and *Hoxb2* differentially control alar and basal plate development within distinct rhombomeres. *Hoxa2*

and *Hoxb2* regulate, in a rhombomere-specific and D-V-restricted manner, the columnar expression patterns of transcription factors involved in the control of neurogenesis and the early specification of subsets of neuronal precursors (Figure 8). Interestingly, the restricted functions of *Hoxa2* and *Hoxb2* along both A-P and D-V axes correlate with their specific rostrocaudal and D-V expression during neurogenesis. Together, these data make the first link between *Hox*-mediated patterning along the A-P axis and neurogenesis along the D-V axis and provide insights into the mechanisms by which neurons are generated at reproducible positions within the hindbrain segments.

Experimental Procedures

Generation of *Hoxb2* and *Hoxa2/Hoxb2* Mutants

The *Hoxb2* targeting construct includes a 7.0 kb XbaI–NotI genomic fragment (Figure 1A). A fragment including a promoterless *lacZ*-polyadenylic acid and a phosphoglycerate kinase–*neo* was inserted in-frame into the exon I, replacing 300 bp of exonic/intronic sequence (NarI–Sall fragment). The targeting vector contains 4.2 kb and 2.5 kb of homologous flanking sequences. The construct was linearized with SclI (a unique site was generated in the vector backbone) prior to electroporation in 129Sv-derived embryonic stem (ES) cells, and DNA from G418-resistant colonies was analyzed by Southern blotting with external probes (Figure 1A). Probes A and B correspond to 600 bp EcoRV–XbaI and 800 bp XbaI–BamHI genomic fragments, respectively. Out of several independent clones carrying the targeted mutation, two (LZ24 and LZ83) were injected into C57BL/6J blastocysts and gave rise to germline chimeric males. Chimeras were crossed with 129Sv females to derive *Hoxb2* mutant mice in a pure genetic background.

The mouse colonies derived from the LZ24 and LZ83 clones displayed undistinguishable phenotypes, and most of the analysis described used the LZ24 line. Mice were genotyped by Southern blotting using probes A and B or by PCR using the UT71/UK4 and UK4/UK6 couple of primers for wild-type and mutant alleles, respectively (Figure 1B). Primer sequences are: UT71, 5'TGGCGGCGGTGACCGCAGAGCAG3'; UK4, 5'CATCGCTCGCCGAGTGTCTGACTTCTTAC3'; and UK6, 5'ATTACGCCAGCTGGCGAAAGGGGATGTGC3'.

Hoxb2 heterozygotes appeared normal and were fertile. The *lacZ* gene failed to be expressed at any of the developmental stages analyzed (8.5, 10.5, and 12.5 dpc). Genotyping of animals derived from heterozygous mutant intercrosses revealed 82% lethality among the homozygotes around birth. Only 60 homozygous mutants out of 1073 animals survived by 3 weeks of age. Of 60, 22 (37%) homozygotes died between 3 weeks and 2 months of age, whereas the surviving homozygous animals had a normal life span and were fertile, although *Hoxb2*^{-/-} females had difficulties raising their pups.

Hoxb2 mutants were crossed with *Hoxa2* mutants (Rijli et al., 1993). A normal Mendelian ratio of double homozygotes was found at birth, showing that these mutants did not die in utero. However, lethality was observed soon after birth, as in the case of single mutants.

In Situ Hybridization and Immunostaining Analysis

Whole-mount in situ hybridizations were performed as described in Gavalas et al. (1998).

Whole-mount immunostaining analysis using the anti-neurofilament (2H3) and anti-ISL1 (4D5) monoclonal antibodies (Developmental Studies Hybridoma Bank) was performed as described in Mark et al. (1993), whereas the anti-KROX-20 polyclonal antibody (BAbCO) was used as described in Goddard et al. (1996).

For each given genotype, experiments using specific antisense probes or antibodies were performed on at least three embryos.

Retrograde Labeling

After fixation in 4% paraformaldehyde in phosphate-buffered saline, embryos were injected with the carbocyanine tracers Dil and DiO (Molecular Probes). Once flat mounted, the retrogradely labeled

hindbrains were analyzed under a confocal microscope (Leica) as described in Studer et al. (1996).

Acknowledgments

We wish to thank J. F. Brunet, M. Ensini, N. S. Foulkes, C. Goridis, F. Guillemot, and S. Nonchev for useful discussions and comments on the manuscript. The help of A. Dierich and M. LeMeur as well as of the ES cell culture and mouse facility staff is gratefully acknowledged. We also thank M. Poulet for excellent technical assistance, Jean-Luc Vonesch and N. Messadeq for help with confocal microscopy, and the following colleagues for probes: P. Charnay (*Krox-20*), R. DiLauro (*Nkx2.2*), P. Gruss (*Pax3*, *Pax6*, *Evx1*), F. Guillemot (*Mash1*, *ngn2*), R. Kageyama (*MATH-3*), D. Wilkinson (*EphA4*), and A. Zelen (*PLZF*). The 2H3 and 4D5 monoclonal antibodies were obtained from the Developmental Studies Hybridoma Bank under contract NO1-HD-7-3263 from the National Institute of Child Health and Human Development. M. D. was supported by a fellowship from La Ligue Nationale Contre le Cancer. M. K. M. was supported by a Medical Research Council Training Fellowship. R. N. was supported by Deutscher Akademischer Austauschdienst and Fondation pour la Recherche Médicale fellowships. This work was supported by grants from l'Institut National de la Santé et de la Recherche Médicale, le Centre National de la Recherche Scientifique, l'Hôpital Universitaire de Strasbourg, and La Ligue Nationale Contre le Cancer. Work in R. K.'s laboratory was supported by the Medical Research Council and a European Economic Community Biotechnology Network grant (BIO2 CT-930060).

Received November 19, 1998; revised February 17, 1999.

References

- Auclair, F., Valdes, N., and Marchand, R. (1996). Rhombomere-specific origin of branchial and visceral motoneurons of the facial nerve in the rat embryo. *J. Comp. Neurol.* **369**, 451–461.
- Barrow, J.R., and Capecchi, M.R. (1996). Targeted disruption of the *Hoxb-2* locus in mice interferes with expression of *Hoxb-1* and *Hoxb-4*. *Development* **122**, 3817–3828.
- Burrill, J.D., Moran, L., Goulding, M.D., and Saueressig, H. (1997). *Pax2* is expressed in multiple spinal cord interneurons, including a population of EN¹⁺ interneurons that require *PAX6* for their development. *Development* **124**, 4493–4503.
- Carpenter, E.M., Goddard, J.M., Chisaka, O., Manley, N.R., and Capecchi, M.R. (1993). Loss of *Hox-A1* (*Hox-1.6*) function results in the reorganization of the murine hindbrain. *Development* **118**, 1063–1075.
- Clarke, J.D., and Lumsden, A. (1993). Segmental repetition of neuronal phenotype sets in the chick embryo hindbrain. *Development* **118**, 151–162.
- Clarke, J.D., Erskine, L., and Lumsden, A. (1998). Differential progenitor dispersal and the spatial origin of early neurons can explain the predominance of single-phenotype clones in the chick hindbrain. *Dev. Dyn.* **212**, 14–26.
- Ensini, M., Tsuchida, T.N., Belting, H.G., and Jessell, T.M. (1998). The control of rostrocaudal pattern in the developing spinal cord: specification of motor neuron subtype identity is initiated by signals from paraxial mesoderm. *Development* **125**, 969–982.
- Ericson, J., Rashbass, P., Schedl, A., Brenner-Morton, S., Kawakami, A., van Heyningen, V., Jessell, T.M., and Briscoe, J. (1997). *Pax6* controls progenitor cell identity and neuronal fate in response to graded *Shh* signaling. *Cell* **90**, 169–180.
- Fode, C., Gradwohl, G., Morin, X., Dierich, A., Le Meur, M., Goridis, C., and Guillemot, F. (1998). The bHLH protein NEUROGENIN 2 is a determination factor for epibranchial placode-derived sensory neurons. *Neuron* **20**, 483–494.
- Fraser, S., Keynes, R., and Lumsden, A. (1990). Segmentation in the chick embryo hindbrain is defined by cell lineage restrictions. *Nature* **344**, 431–435.
- Gavalas, A., Davenne, M., Lumsden, A., Chambon, P., and Rijli, F.M.

- (1997). Role of *Hoxa-2* in axon pathfinding and rostral hindbrain patterning. *Development* **124**, 3693–3702.
- Gavalas, A., Studer, M., Lumsden, A., Rijli, F.M., Krumlauf, R., and Chambon, P. (1998). *Hoxa1* and *Hoxb1* synergize in patterning the hindbrain, cranial nerves and second pharyngeal arch. *Development* **125**, 1123–1136.
- Goddard, J.M., Rossel, M., Manley, N.R., and Capecchi, M.R. (1996). Mice with targeted disruption of *Hoxb-1* fail to form the motor nucleus of the VIIIth nerve. *Development* **122**, 3217–3228.
- Gould, A., Itasaki, N., and Krumlauf, R. (1998). Initiation of rhombomeric *Hoxb4* expression requires induction by somites and a retinoid pathway. *Neuron* **21**, 39–51.
- Goulding, M.D., Lumsden, A., and Gruss, P. (1993). Signals from the notochord and floor plate regulate the region-specific expression of two Pax genes in the developing spinal cord. *Development* **117**, 1001–1016.
- Gradwohl, G., Fode, C., and Guillemot, F. (1996). Restricted expression of a novel murine atonal-related bHLH protein in undifferentiated neural precursors. *Dev. Biol.* **180**, 227–241.
- Graham, A., Maden, M., and Krumlauf, R. (1991). The murine Hox-2 genes display dynamic D-V patterns of expression during central nervous system development. *Development* **112**, 255–264.
- Grapin-Botton, A., Bonnin, M.A., and Le Douarin, N.M. (1997). Hox gene induction in the neural tube depends on three parameters: competence, signal supply and paralogue group. *Development* **124**, 849–859.
- Guillemot, F., and Joyner, A.L. (1993). Dynamic expression of the murine Achaete-Scute homologue Mash-1 in the developing nervous system. *Mech. Dev.* **42**, 171–185.
- Guthrie, S., and Lumsden, A. (1991). Formation and regeneration of rhombomere boundaries in the developing chick hindbrain. *Development* **112**, 221–229.
- Hirsch, M.R., Tiveron, M.C., Guillemot, F., Brunet, J.F., and Goridis, C. (1998). Control of noradrenergic differentiation and *Phox2a* expression by MASH1 in the central and peripheral nervous system. *Development* **125**, 599–608.
- Irving, C., Nieto, M.A., Das Gupta, R., Charnay, P., and Wilkinson, D.G. (1996). Progressive spatial restriction of *Sek-1* and *Krox-20* gene expression during hindbrain segmentation. *Dev. Biol.* **173**, 26–38.
- Itasaki, N., Sharpe, J., Morrison, A., and Krumlauf, R. (1996). Reprogramming *Hox* expression in the vertebrate hindbrain: influence of paraxial mesoderm and rhombomere transposition. *Neuron* **16**, 487–500.
- Kageyama, R., and Nakanishi, S. (1997). Helix–loop–helix factors in growth and differentiation of the vertebrate nervous system. *Curr. Opin. Genet. Dev.* **7**, 659–665.
- Lo, L.C., Johnson, J.E., Wuenschell, C.W., Saito, T., and Anderson, D.J. (1991). Mammalian achaete-scute homolog 1 is transiently expressed by spatially restricted subsets of early neuroepithelial and neural crest cells. *Genes. Dev.* **5**, 1524–1537.
- Lo, L., Tiveron, M.C., and Anderson, D.J. (1998). MASH1 activates expression of the paired homeodomain transcription factor *Phox2a*, and couples pan-neuronal and subtype-specific components of autonomic neuronal identity. *Development* **125**, 609–620.
- Lumsden, A., and Keynes, R. (1989). Segmental patterns of neuronal development in the chick hindbrain. *Nature* **337**, 424–428.
- Lumsden, A., and Krumlauf, R. (1996). Patterning the vertebrate neuraxis. *Science* **274**, 1109–1115.
- Lumsden, A., Clarke, J.D., Keynes, R., and Fraser, S. (1994). Early phenotypic choices by neuronal precursors, revealed by clonal analysis of the chick embryo hindbrain. *Development* **120**, 1581–1589.
- Ma, Q., Sommer, L., Cserjesi, P., and Anderson, D.J. (1997). Mash1 and neurogenin1 expression patterns define complementary domains of neuroepithelium in the developing CNS and are correlated with regions expressing notch ligands. *J. Neurosci.* **17**, 3644–3652.
- Maconochie, M.K., Nonchev, S., Studer, M., Chan, S.K., Popperl, H., Sham, M.H., Mann, R.S., and Krumlauf, R. (1997). Cross-regulation in the mouse HoxB complex: the expression of *Hoxb2* in rhombomere 4 is regulated by *Hoxb1*. *Genes. Dev.* **11**, 1885–1895.
- Marin, F., and Puelles, L. (1995). Morphological fate of rhombomeres in quail/chick chimeras: a segmental analysis of hindbrain nuclei. *Eur. J. Neurosci.* **7**, 1714–1738.
- Mark, M., Lufkin, T., Vonesch, J.L., Ruberte, E., Olivo, J.C., Dolle, P., Gorry, P., Lumsden, A., and Chambon, P. (1993). Two rhombomeres are altered in *Hoxa-1* mutant mice. *Development* **119**, 319–338.
- Marshall, H., Nonchev, S., Sham, M.H., Muchamore, I., Lumsden, A., and Krumlauf, R. (1992). Retinoic acid alters hindbrain Hox code and induces transformation of rhombomeres 2/3 into a 4/5 identity. *Nature* **360**, 737–741.
- McKay, I.J., Lewis, J., and Lumsden, A. (1997). Organization and development of facial motor neurons in the kreisler mutant mouse. *Eur. J. Neurosci.* **9**, 1499–1506.
- Nonchev, S., Vesque, C., Maconochie, M., Seitanidou, T., Ariza-McNaughton, L., Frain, M., Marshall, H., Sham, M.H., Krumlauf, R., and Charnay, P. (1996). Segmental expression of *Hoxa-2* in the hindbrain is directly regulated by *Krox-20*. *Development* **122**, 543–554.
- Osumi, N., Hirota, A., Ohuchi, H., Nakafuku, M., Iimura, T., Kuratani, S., Fujiwara, M., Noji, S., and Eto, K. (1997). Pax-6 is involved in the specification of hindbrain motor neuron subtype. *Development* **124**, 2961–2972.
- Pattyn, A., Morin, X., Cremer, H., Goridis, C., and Brunet, J.F. (1997). Expression and interactions of the two closely related homeobox genes *Phox2a* and *Phox2b* during neurogenesis. *Development* **124**, 4065–4075.
- Pfaff, S., and Kintner, C. (1998). Neuronal diversification: development of motor neuron subtypes. *Curr. Opin. Neurobiol.* **8**, 27–36.
- Rijli, F.M., Mark, M., Lakkaraju, S., Dierich, A., Dolle, P., and Chambon, P. (1993). A homeotic transformation is generated in the rostral branchial region of the head by disruption of *Hoxa-2*, which acts as a selector gene. *Cell* **75**, 1333–1349.
- Rijli, F.M., Gavalas, A., and Chambon, P. (1998). Segmentation and specification in the branchial region of the head: the role of the Hox selector genes. *Int. J. Dev. Biol.* **42**, 393–401.
- Roztocil, T., Matter-Sadzinski, L., Alliod, C., Ballivet, M., and Matter, J.M. (1997). NeuroM, a neural helix–loop–helix transcription factor, defines a new transition stage in neurogenesis. *Development* **124**, 3263–3272.
- Schneider-Maunoury, S., Seitanidou, T., Charnay, P., and Lumsden, A. (1997). Segmental and neuronal architecture of the hindbrain of *Krox-20* mouse mutants. *Development* **124**, 1215–1226.
- Sham, M.H., Vesque, C., Nonchev, S., Marshall, H., Frain, M., Gupta, R.D., Whiting, J., Wilkinson, D., Charnay, P., and Krumlauf, R. (1993). The zinc finger gene *Krox20* regulates *HoxB2* (*Hox2.8*) during hindbrain segmentation. *Cell* **72**, 183–196.
- Simon, H., and Lumsden, A. (1993). Rhombomere-specific origin of the contralateral vestibulo-acoustic efferent neurons and their migration across the embryonic midline. *Neuron* **11**, 209–220.
- Simon, H., Hornbruch, A., and Lumsden, A. (1995). Independent assignment of antero-posterior and dorso-ventral positional values in the developing chick hindbrain. *Curr. Biol.* **5**, 205–214.
- Sommer, L., Ma, Q., and Anderson, D.J. (1996). Neurogenins, a novel family of atonal-related bHLH transcription factors, are putative mammalian neuronal determination genes that reveal progenitor cell heterogeneity in the developing CNS and PNS. *Mol. Cell. Neurosci.* **8**, 221–241.
- Stoykova, A., Gotz, M., Gruss, P., and Price, J. (1997). Pax6-dependent regulation of adhesive patterning, R-cadherin expression and boundary formation in developing forebrain. *Development* **124**, 3765–3777.
- Stuart, E.T., Kioussi, C., and Gruss, P. (1994). Mammalian Pax genes. *Annu. Rev. Genet.* **28**, 219–236.
- Studer, M., Lumsden, A., Ariza-McNaughton, L., Bradley, A., and Krumlauf, R. (1996). Altered segmental identity and abnormal migration of motor neurons in mice lacking *Hoxb-1*. *Nature* **384**, 630–634.
- Studer, M., Gavalas, A., Marshall, H., Ariza-McNaughton, L., Rijli, F.M., Chambon, P., and Krumlauf, R. (1998). Genetic interactions between *Hoxa1* and *Hoxb1* reveal new roles in regulation of early hindbrain patterning. *Development* **125**, 1025–1036.

- Takebayashi, K., Takahashi, S., Yokota, C., Tsuda, H., Nakanishi, S., Asashima, M., and Kageyama, R. (1997). Conversion of ectoderm into a neural fate by ATH-3, a vertebrate basic helix-loop-helix gene homologous to *Drosophila* proneural gene *atonal*. *EMBO J.* *16*, 384–395.
- Tanabe, Y., and Jessell, T.M. (1996). Diversity and pattern in the developing spinal cord. *Science* *274*, 1115–1123.
- Theil, T., Frain, M., Gilardi-Hebenstreit, P., Flenniken, A., Charnay, P., and Wilkinson, D.G. (1998). Segmental expression of the EphA4 (Sek-1) receptor tyrosine kinase in the hindbrain is under direct transcriptional control of *Krox-20*. *Development* *125*, 443–452.
- Tiret, L., Le Mouellic, H., Maury, M., and Brulet, P. (1998). Increased apoptosis of motoneurons and altered somatotopic maps in the brachial spinal cord of *Hoxc-8*-deficient mice. *Development* *125*, 279–291.
- Wizenmann, A., and Lumsden, A. (1997). Segregation of rhombomeres by differential chemoaffinity. *Mol. Cell. Neurosci.* *9*, 448–459.
- Wolpert, L. (1969). Positional information and the spatial pattern of cellular differentiation. *J. Theor. Biol.* *25*, 1–47.
- Xu, Q., Alldus, G., Holder, N., and Wilkinson, D.G. (1995). Expression of truncated *Sek-1* receptor tyrosine kinase disrupts the segmental restriction of gene expression in the *Xenopus* and zebrafish hindbrain. *Development* *121*, 4005–4016.
- Ye, W., Shimamura, K., Rubenstein, J.L., Hynes, M.A., and Rosenthal, A. (1998). FGF and Shh signals control dopaminergic and serotonergic cell fate in the anterior neural plate. *Cell* *93*, 755–766.
- Zhang, M., Kim, H.J., Marshall, H., Gendron-Maguire, M., Lucas, D.A., Baron, A., Gudas, L.J., Gridley, T., Krumlauf, R., and Grippo, J.F. (1994). Ectopic *Hoxa-1* induces rhombomere transformation in mouse hindbrain. *Development* *120*, 2431–2442.